Plant-activated bacterial receptor adenylate cyclases modulate epidermal infection in the *Sinorhizobium meliloti–Medicago* symbiosis

Chang Fu Tian[a,b,c,1], Anne-Marie Garnerone[a,b,1], Céline Mathieu-Demazière[a,b], Catherine Masson-Boivin[a,b], and Jacques Batut[a,b,2]

[a]Laboratoire des Interactions Plantes-Microorganismes, Institut National de la Recherche Agronomique, Unité Mixte de Recherche 441, F-31326 Castanet-Tolosan, France; [b]Laboratoire des Interactions Plantes-Microorganismes, Centre National de la Recherche Scientifique, Unité Mixte de Recherche 2594, F-31326 Castanet-Tolosan, France; and [c]State Key Laboratory of Agrobiotechnology, College of Biological Sciences, China Agricultural University, Beijing 100193, China

Legumes and soil bacteria called rhizobia have coevolved a facultative nitrogen-fixing symbiosis. Establishment of the symbiosis requires bacterial entry via root hair infection threads and, in parallel, organogenesis of nodules that subsequently are invaded by bacteria. Tight control of nodulation and infection is required to maintain the mutualistic character of the interaction. Available evidence supports a passive bacterial role in nodulation and infection after the microsymbiont has triggered the symbiotic plant developmental program. Here we identify in *Sinorhizobium meliloti*, the *Medicago* symbiont, a cAMP-signaling regulatory cascade consisting of three receptor-like adenylate cyclases, a Crp-like regulator, and a target gene of unknown function. The cascade is activated specifically by a plant signal during nodule organogenesis. Cascade inactivation results in a hyperinfection phenotype consisting of abortive epidermal infection events uncoupled from nodulation. These findings show that, in response to a plant signal, rhizobia play an active role in the control of infection. We suggest that rhizobia may modulate the plant's susceptibility to infection. This regulatory loop likely aims at optimizing legume infection.

Rhizobia are phylogenetically diverse bacteria that have achieved the ability to enter a nitrogen-fixing symbiosis with legumes (1). Rhizobia elicit the formation on roots of legume host plants of new organs called "nodules," which rhizobia colonize intracellularly and in which they fix atmospheric nitrogen, to the benefit of the plant. The best-described mode of rhizobia entry into plant roots involves the formation of specific tubular structures called "infection threads" (ITs) that rhizobia initiate at the tip of susceptible root hairs. Extension and branching of ITs in direction of the root cortex ensures bacterial colonization of the forming nodule primordium. Ultimately, rhizobia leave ITs to form intracellular structures called "symbiosomes" that acquire competence in biological nitrogen fixation.

Nodule morphogenesis and rhizobial infection are tightly coordinated, although genetically dissectible, processes (2, 3). Flavonoid compounds present in legume root exudates combined with the rhizobial NodD transcriptional regulator(s) induce the synthesis of substituted lipochitooligosaccharides called "Nod factors," which are required for nodule organogenesis and IT formation (3, 4). Additional bacterial molecules, such as low-molecular-weight exopolysaccharides, are required for IT elongation. However, their mode of action has not been elucidated thus far (5).

Available evidence indicates that the microsymbiont, after it has initiated the plant developmental program, has a passive role in the interaction that is dominated by the plant (3). Nodule number is regulated negatively by a variety of mechanisms including the systemic autoregulation of nodulation that involves signaling by CLE peptides (6–8). Bacterial infection of root tissues is controlled by the plant at the epidermal cell layer in close coordination with nodule development (2, 9). Hyperinfection, usually associated with abnormal nodule development, has been described in a few

legume mutants (9–11). Finally, cysteine-rich plant peptides strictly control bacteroid proliferation and differentiation in galegoid legumes (12).

Here we report a slightly contrasting pattern in the *Sinorhizobium meliloti–Medicago* symbiosis, showing that the control of epidermal infection actually involves a sustained molecular dialogue between the two partners. Specifically, we have found that a plant signal activates a cAMP regulatory cascade in *S. meliloti* that, in turn, modulates the extent of epidermal infection, possibly by modifying the plant susceptibility to infection.

Results

Characterization of a cAMP Signal Transduction Cascade in *S. meliloti*. *S. meliloti* sequencing revealed the occurrence of 26 type III purine nucleotidyl (adenylate and guanylate) cyclases in the genome (13). CyaD1 (SMc02176), CyaD2 (SMc04307), and CyaK (SMb20776) share the following structural organization: an amino-terminal signal peptide, a CHASE2 extracellular domain (IPR007890) (14), a set of three membrane-spanning domains, and a cytoplasmic catalytic domain (IPR001054) characteristic of type III adenylate cyclase/guanylate cyclase (AC/GC) enzymes. To characterize the substrate specificity of these putative cyclases, we measured cAMP and cGMP levels in vivo in the wild-type *S. meliloti* strain and in a *cyaD1D2K* triple mutant. In the wild-type strain, cAMP levels were *ca.* 20-fold higher than cGMP levels in vivo. Neither was affected by the simultaneous inactivation of all three cyclases, possibly because of functional redundancy. Instead, expression of a truncated form of CyaD1 in which the periplasmic CHASE2 domain was deleted in frame (pGMI50127; see Table S2) provoked a significant increase in cAMP content in *S. meliloti* cell extracts (Fig. 1). This increase was consistent with CyaD1 acting in vivo as an AC, possibly with a GC side activity, like most type III enzymes described so far (15). Sequence alignment of CyaD1, CyaD2, and CyaK with well-characterized ACs and GCs showed that a lysine residue (K56 in CyaD1) that is specifically conserved in ACs (16) is conserved in all three cyclases (Fig. S1), thus suggesting that CyaD2 and CyaK also are ACs.

Next to *cyaD1* on the *S. meliloti* chromosome, we identified a Crp-like transcriptional regulator (Clr; Smc02175) as well as a
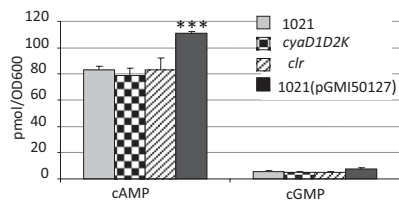
Fig. 1. Functional characterization of the CyaD1 protein. ELISA measurements of intracellular cAMP and cGMP levels in *S. meliloti* strains 1021, *cyaD1D2K*, and *clr* and in the *cyaD1ΔCHASE2*-expressing derivative 1021 (pGMI50127). ***$P < 0.001$.

gene of unknown function, *smc02178*, that we have found to be a target gene for *clr*. Clr belongs to a family of 13 Crp-like proteins in *S. meliloti* that includes the FixK regulators of microoxic respiration and nitrogen-fixation genes whose activity is cAMP independent (17). Instead, the conservation in Clr of residues that bind cAMP in *Escherichia coli* CRP and other characterized cAMP-binding proteins (Fig. S2) predicted that Clr would be a cAMP-binding protein. We have found that *clr* is not involved in catabolite repression by succinate in *S. meliloti*.

A *smc02178-lacZ* reporter gene fusion was expressed at a very low level in free-living conditions in either synthetic Vincent medium (Fig. 2) or complex [tryptone-yeast extract (TY) or LB medium]. High expression could be driven by exogenously provided cAMP, in a *clr*-dependent manner, independently of *cyaD1cyaD2cyaK* (Fig. 2*A*). Similarly, endogenous production of cAMP by the plasmid construct pGMI50127 (*cyaD1ΔCHASE2*) led to high constitutive expression of the *smc02178* target gene (Fig. 2*B*). Taken together, these data identify a regulatory cascade in which activated CyaD1, CyaD2, and CyaK cyclases produce cAMP that, together with the Clr transcriptional regulator, drives *smc02178* gene expression.

Plant Signal Triggers Symbiotic Activation of the Cascade. Expression of the *smc02178-lacZ* reporter gene fusion was observed in a *S. meliloti* 1021 wild-type background in all infected parts of young [7 d postinfection (dpi)] and mature (14 dpi) nodules of *Medicago sativa* (Fig. 3 *A* and *F*). By contrast, *smc02178-lacZ* expression was rarely observed in epidermal ITs. Inactivation of the *clr* gene or triple *cyaD1D2K* inactivation abolished expression of the *smc02178-lacZ* fusion in nodules (Fig. 3 *B*, *C*, *G*, and *H*). Individual inactivation of *cyaD1*, *cyaD2*, and *cyaK* or simultaneous inactivation of *cyaD1* and *cyaD2* had a partial effect on *smc02178-lacZ* expression in nodules (Fig. 3 *D*, *E*, *I*, and *J*), thus indicating that all three cyclases contribute to symbiotic activation.

Nodule crude extracts prepared from 14-dpi-old nodules formed by a wild-type *S. meliloti* strain induced high expression of
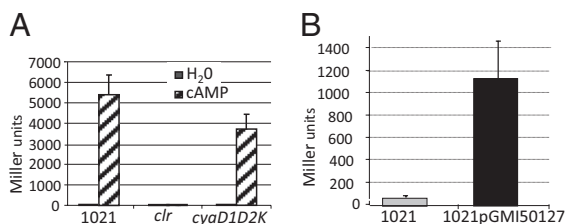

Fig. 2. cAMP drives *clr*-dependent activation of the *smc02178-lacZ* reporter gene fusion *ex planta*. cAMP was provided either exogenously (*A*) or endogenously by the constitutive *cyaD1ΔCHASE2*-expressing plasmid pGMI50127 (*B*). *smc02178-lacZ* activity in *S. meliloti* 1021, *clr*, and *cyaD1D2K* strains and in the *cyaD1ΔCHASE2*-expressing strain (1021 pGMI50127) is expressed in Miller units. Error bars indicate SE; *n* = 3. The mean value difference between strain 1021 and the *cyaD1D2K* mutant in *A* was not statistically significant (*t* = 0.07).

the *smc02178-lacZ* reporter gene fusion *ex planta* in a *S. meliloti* 1021 wild-type genetic background (Fig. 4*A*). Activation did not occur in either a *clr* mutant background or in a *cyaD1D2K* triple mutant (Fig. 4*A*) that excluded activation by the cAMP potentially present in nodules (18). This result suggested that a bona fide inducing signal was present in nodule extracts. *Medicago* root exudates, the nodulation gene inducer luteolin (4), cytokinin, or proline had no detectable effect on *smc02178-lacZ* expression. Similarly, low oxygen (19), high sucrose, or NaCl concentrations had no effect. No signaling activity could be detected in non-nodulated portions of inoculated roots or in noninoculated roots of *M. sativa* (Fig. 4*A*). By contrast, signaling activity was detected in shoots of both inoculated and noninoculated plants but at a lower specific activity than in nodules (Fig. 4*A*).

High inducing activity was present in sterile, spontaneous nodules formed by the nodulation in the absence of rhizobia (Nar) variant of *M. sativa* (Fig. 4*B*) (20), thus showing that the signal was of plant origin. Signal activity also was detected in noninvaded nodules induced by the exopolysaccharide-defective *exoY* mutant of *S. meliloti* (21) (Fig. S3). Hence signal presence in wild-type *Medicago* nodules did not require infection by bacteria.

High signaling activity also was detected in nodule and shoot extracts from pea and lotus as well as in the shoots of nonlegumes such as rice (Fig. S4).

Cascade Mutants Are Hyperinfective in *M. sativa*. The *cyaD1D2K*, *clr*, and *smc02178*-null mutants induced normal, elongated, pink nodules with the same early kinetics as wild-type 1021. No significant increase in nodule number was observed over a large set of independent experiments (Figs. 5*A* and 6*A*; also see Fig. S6). The *cyaD1D2K* mutant's nitrogen-fixation ability (as measured by acetylene-reduction assay) and whole-plant growth yield of plants (dry weight) were not statistically different from wild type (Fig. S5). Instead, a distinctive phenotype of the *cyaD1D2K*, *clr*, and *smc02178* mutants was a three- to fourfold increase in the total number of epidermal ITs formed. This increase was statistically highly significant ($P < 0.001$) at 14 dpi (Fig. 5*A*) but could be observed as early as 7 dpi, although with more variation (Fig. S6). As a control, we monitored infection by the *S. meliloti* *ccmA* mutant that is completely defective in nitrogen fixation (22). The *ccmA* mutant formed significantly more nodules than wild type, as expected for a Fix⁻ mutant, but did not display a hyperinfection phenotype (Fig. 5*A*), thus ruling out the possibility that hyperinfection could result from a slight decrease in nitrogen-fixation efficiency. Complementation assays confirmed that the hyperinfective phenotype was linked genetically to the *clr* mutation (Fig. 5*A*). Simultaneous inactivation of *cyaD1* and *cyaD2* led to an intermediate hyperinfection phenotype (Fig. 5*A*; $P < 0.01$), whereas inactivation of *cyaK* alone had no detectable effect, thus suggesting that the three cyclases contribute to the control of infection.

The superfluous ITs typically elongated over the entire root hair length but aborted at the interface between the epidermis and the cortex with associated defense reactions (Fig. 5*G* and Fig. S7). They occurred on roots irrespective of the presence of nodule primordium (Fig. 5 *B–D*). Nodules with multiple infection foci, a feature that we never observed in the wild-type strain, sometimes were observed (Fig. 5*F*). Taken together, these findings indicated that hyperinfection is uncoupled from nodule formation. Finally, compared with wild type, the mutants initiated more abortive ITs outside the portion of the root that normally is susceptible to primary infection (23), including on lateral roots (Fig. 5*E* and Fig. S7).

Bacterial cAMP Cascade May Modulate Plant Susceptibility to Infection. To compare the symbiotic performances of the wild type and *clr* mutant, we coinoculated them (1/1 ratio) on *M. sativa* seedlings after labeling the strains with RFP or GFP fluorescent tags (see
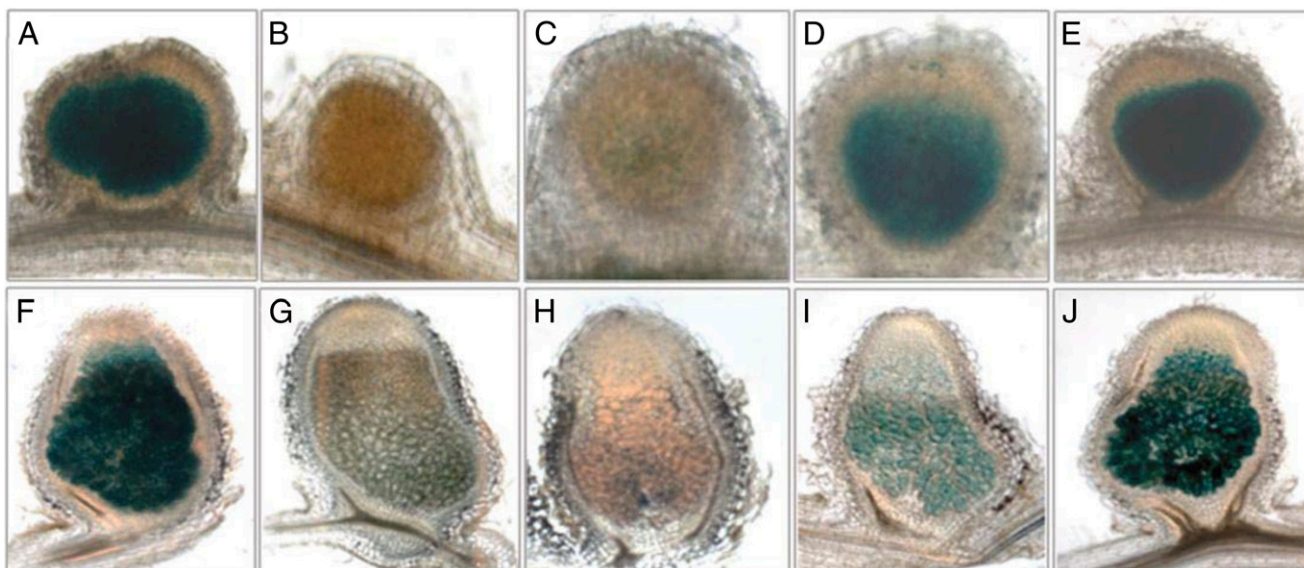
Fig. 3. Expression of the *smc02178-lacZ* reporter gene fusion in *M. sativa* nodules. Nodules were observed at 7 dpi (*A–E*) and 14 dpi (*F–J*) after inoculation with *S. meliloti* 1021 (*A* and *F*), *clr* (*B* and *G*), *cyaD1D2K* (*C* and *H*), *cyaK* (*D* and *I*), and *cyaD1D2* strains (*E* and *J*) carrying pGD2178.

). The numbers of nodules and abortive ITs initiated by each strain were recorded at 14 dpi (Fig. 6). We verified by swapping experiments that the tags did not influence results.

Nodule number was the same for the wild-type and *clr* strains and did not change upon coinoculation (Fig. 6*A*), thus confirming that inactivation of the cAMP-signaling cascade had no effect on nodulation. This result also indicated that the two strains had the same competitiveness for nodulation and did not differ in their ability to initiate primary infection events, i.e., the formation of productive ITs leading to nodule formation. Upon coinoculation, the number of abortive ITs initiated by the *clr* strain was not higher than that initiated by the wild-type strain, as would be expected if the *clr* strain had a better infectiveness (Fig. 6*B*). Instead, the number of ITs initiated by the wild-type strain increased significantly upon coinoculation with the *clr* mutant, so as to match the inoculation ratio (1/1). Conversely, the number of ITs initiated by the *clr* mutant decreased in the presence of the wild-type strain. Taken together, these findings indicate that the plant did not discriminate between the wild-type and the *clr* mutant strains for infection. Because of the very low inoculum load (4.10^2 bacteria of each strain per plantlet), it is highly unlikely that the two strains could complement each other extracellularly, and, indeed, colocalized bacteria were not observed on roots. Instead, these data suggest that the bacterial cAMP cascade may modulate the plant's sensitivity to infection. Interestingly, the repartition of abortive ITs initiated by the wild-type strain along the root now matched that of the *clr* mutant, a finding that also suggests an altered sensitivity of the plant root.

Discussion

We have shown here activation by a plant signal of a cAMP cascade in bacteria that are colonizing the forming nodule. Genetic inactivation of the cAMP cascade led to hyperinfection of plant roots, thus suggesting that the biological function of the cAMP cascade is to keep root-hair infection (IT formation) under control. To summarize our findings, we propose a working model in which the cAMP regulatory cascade is activated in bacteria that have penetrated nodule tissues successfully. Activation of this cAMP cascade, in turn, would restrict further infection by external, rhizospheric bacteria by a mechanism that remains to be elucidated (Fig. 7). Inactivation of the cAMP cascade may increase intrinsic bacterial infectiveness or, alternatively, may enhance the root's susceptibility to infection. Although the two possibilities remain open, we presently favor the second hypothesis, because it accounts more readily for all our observations: (*i*) it explains how activation of the cAMP cascade in bacteria that already have penetrated
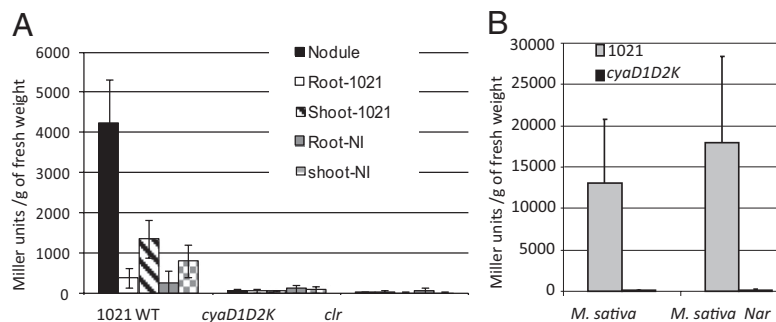

Fig. 4. A plant signal triggers activation of the cAMP cascade in nodules. *smc02178-lacZ* expression was monitored *ex planta* in 1021, *clr*, and *cyaD1D2K* background strains after addition of *M. sativa* tissue extracts. (*A*) Extracts of nodules or nonnodulated portions of roots and shoots inoculated with *S. meliloti* 1021 or shoot and root extracts of noninoculated (NI) plants. (*B*) Bacteria-free nodule extracts of the spontaneously nodulating *M. sativa* Nar variant trigger cascade activation *ex planta*.
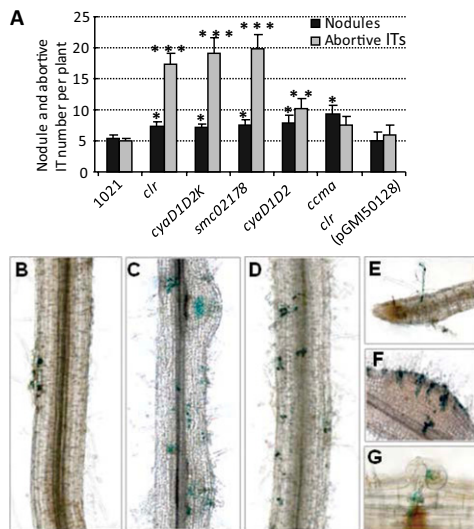
Fig. 5. Symbiotic phenotypes of cAMP-cascade mutants on *M. sativa*. (*A*) Total number of nodules and total number of ITs formed outside nodules (abortive ITs) at 14 dpi on *M. sativa* inoculated with 1021 and various mutants, including a *ccmA* Fix⁻ mutant and the complemented *clr*(pGMI50128) mutant strain, all carrying a constitutive *hemA-lacZ* reporter gene fusion (pXLGD4) for visualization. Data were collected from three independent experiments with 10 plants inoculated per bacterial strain. *P* < 0.05; **P < 0.01; ***P < 0.001. (*B–G*) *M. sativa* seedlings were inoculated with 1021 (*B*), *cyaD1D2K* (*C*), *clr* (*D* and *F*), or *smc02178* (*G*) mutants. Multiple infection loci (colored blue) were initiated by mutants along the main root at 7 dpi (*B–D*) and in a 7-dpi nodule (*F*). Note the absence of nodule primordium in *D*. IT formation near the tip of a lateral root is shown in *E*. Abortive ITs with associated defense reactions (brown accumulation of polyphenolics) were visible at 14 dpi in *G*. (Magnification: *B–D*, 10×; *E* and *F*, 20×; *G*, 30×.)

nodule tissues may influence infection by external, rhizospheric rhizobia; (*ii*) it is consistent with the observation that the plant did not discriminate between wild-type bacteria and the *clr* mutant in coinoculation experiments under conditions where extracellular complementation was unlikely; (*iii*) it is consistent with the increased occurrence of infection events at atypical locations of the root upon inoculation with cAMP-cascade mutants or upon coinoculation with the wild-type strain and the *clr* mutant (although this increase could not be quantified precisely). A longer-lasting susceptibility of the plant to infection after inoculation with cAMP-cascade mutants and/or a spatial modulation of the root susceptibility to infection may account for our observations. However, further experiments, including the identification and precise localization of the plant signal in nodules/infected roots as well as the elucidation of the mode of action of the SMc02178 protein, are needed to discriminate definitely between an enhanced infectiveness of cAMP-cascade mutants and/or an enhanced sensitivity of the plant. Whatever the mechanism at work, we speculate that this regulatory loop may have evolved as a sophistication of the symbiotic interaction toward mutualism by optimizing the extent of IT formation and preventing spurious infection events once a sufficient number of neo-formed nodules has been infected successfully.

Signal exchange is central to the establishment and maintenance of the mutualistic interaction between the two partners. Legume signals described so far include flavonoids as elicitors of bacterial *nod* gene expression (4) and peptides as regulators of nodulation and bacteroid differentiation (24). The results reported here provide evidence of another instance of signaling in this symbiosis. The plant signal was detected in nodules and shoots but could not be detected in roots, whether inoculated or not. This observation argues against signal translocation from shoots to nodules and, instead, tends to support signal synthesis
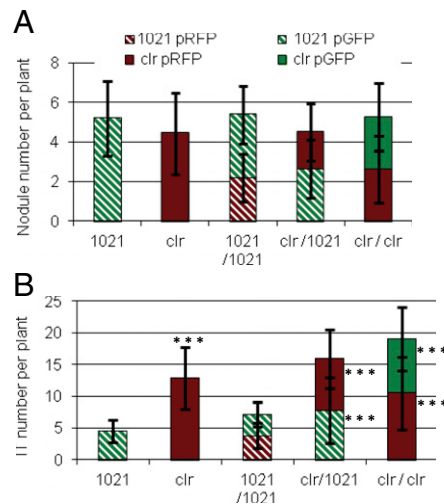

Fig. 6. Coinoculation experiments of wild-type and *clr* mutant strains. Nodule (*A*) and abortive IT (*B*) numbers in coinoculation experiments (1/1 ratio) of the wild-type and *clr* mutant strains at 14 dpi. *M. sativa* seedlings were inoculated with bacteria (4.10²) of either strain labeled with a GFP or RFP tag (Table S2). Data were collected from three independent experiments with 10 plants inoculated per bacterial strain. Statistical significance (***P < 0.001) is shown with respect to strain 1021 alone.

during nodule organogenesis. Biochemical identification of the signal molecule and analysis of the regulation of the gene(s) controlling its synthesis should shed light on the link between signal synthesis, nodule organogenesis, and, possibly, Nod factor signaling. How endosymbiotic bacteria sense the plant signal also remains to be elucidated. Our data suggest that the periplasmic regulatory CHASE2 domain, whose truncation resulted in constitutive activation of the CyaD1 cyclase, contributes to signal sensing, either upon direct interaction with the plant signal molecule itself or indirectly via additional receptor proteins. The specificity of cAMP signaling in *S. meliloti* also is an intriguing issue, given the high number of ACs in this bacterium. Cellular compartmentalization of cAMP in microdomains may contribute to specificity, as suggested in other systems (25).

Little is known so far about cAMP signaling in the context of plant–microbe interactions. However, cAMP signaling is known
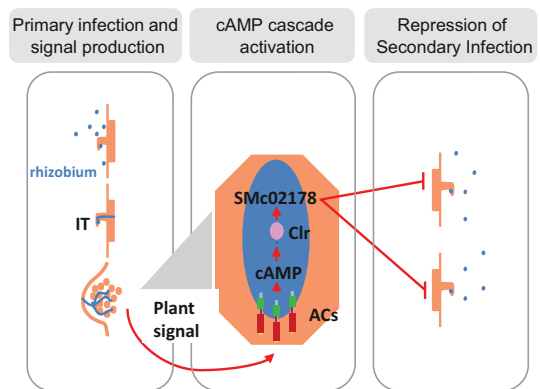

Fig. 7. Model for the bacterial control of IT formation. Rhizobia (blue) trigger initial IT formation and nodule organogenesis on susceptible host plants. A plant signal synthesized during nodule organogenesis promotes activation of the cAMP cascade in endosymbiotic rhizobia. Activation of the bacterial cAMP cascade in turn inhibits secondary IT formation by rhizospheric bacteria. Genetic disruption of the cascade results in abortive epidermal hyperinfection uncoupled from nodulation.

to play a major role in the interaction between animal pathogens and their eukaryotic hosts. In those cases, cAMP signaling serves two complementary functions (reviewed in ref. 26). First, it coordinates virulence gene expression with host environment cues. Second, it suppresses host immune responses by manipulating host cAMP-signaling pathways, either by injection of AC toxins and/or effector molecules or by direct secretion of cAMP into macrophages (26). Functional studies of the SMc02178 protein should shed light to the mechanism(s) at work in *S. meliloti*. The contribution of cAMP signaling to plant–microbe interactions thus may attract further interest in the near future.

Materials and Methods

Bacterial Strains, Plasmids, and Growth Conditions. Bacterial strains and plasmids used in this study are listed in Tables S1 and S2, respectively. *S. meliloti* strains were grown at 28 °C in rich LB medium supplemented with 2.5 mM CaCl$_2$ and 2.5 mM MgSO$_4$, or in modified Vincent synthetic medium with glutamate (0.1%) and mannitol (1%) as nitrogen and carbon sources, respectively (VGM) (27), or in M9 minimal medium with succinate (0.2%) as the carbon source (28). The concentrations of antibiotics used for *S. meliloti* cultures were 200 µg/mL for streptomycin, 100 µg/mL for neomycin, 10 µg/mL for tetracycline, and 30 µg/mL for gentamicin.

Construction of Plasmids and Mutant Strains. Primers used for DNA amplification are listed in Table S3. *S. meliloti 1021* was used as template for DNA amplification. The *cyaD1*, *clr*, and *smc02178* single mutants (GMI11561 GMI11567, and GMI11566, respectively) were constructed by site-specific insertional inactivation using the plasmid pVO155 that does not replicate in *S. meliloti* (29). *cyaD1*, *clr*, and *smc02178* internal PCR fragments were amplified using D1L-D1R, X2175-B2175, and B2178H-X2178B primers, respectively, cloned into pCR2-1-TOPO and then digested with BamHI and XbaI for cloning into pVO155. The resulting pVO155 derivatives were introduced into *E. coli* by transformation and then were conjugated in *S. meliloti*. pVO155 integration at the homologous site in *S. meliloti* was verified by Southern blot analysis.

For deletion of the *cyaD2* and *cyaK* genes, we used the cre-lox system (30). PCR fragments encompassing the upstream/amino-terminal coding region and the downstream/carboxyl-terminal coding region of *cyaD2* were amplified using D2upL-D2upR and D2downL-D2downR as primers (Table S3), digested by EcoRI-KpnI and ApaI-SacI, and cloned into the EcoRI-KpnI and ApaI-SacI restriction sites of pCM351, respectively. The resulting plasmid was introduced into the *S. meliloti 1021 cyaD1* mutant (GMI11561) by conjugation. Transconjugants sensitive to tetracycline and resistant to gentamicin were screened. A *cyaD1 cyaD2* double-mutant GMI11557 was selected, into which the plasmid pCM157 expressing Cre recombinase was introduced by conjugation. Transconjugants sensitive to gentamicin were screened. Subsequently, pCM157 was cured by screening for tetracycline-sensitive strains. Similarly, the upstream 5′-coding end and the downstream 3′-coding end regions of *cyaK* were amplified using KupL-KupR and KdownL-KdownR as primers, were digested by PvuII-KpnI and ApaI-SacI, and were cloned sequentially into the PvuII-KpnI and ApaI-SacI restriction sites of pCM351, respectively. The resulting plasmid then was introduced into the *S. meliloti cyaD1cyaD2* double mutant (GMI11557) or into the *1021* wild-type strain by conjugation. Transconjugants resistant to gentamicin and sensitive to tetracycline were screened. A *cyaD1cyaD2cyaK* triple mutant was selected as GMI11558, and a *cyaK* mutant was selected as GMI11556 (Table S1).

For the construction of the *cyaD1ΔCHASE2*-expressing plasmid pGIMI50127 (Table S2), the upstream/amino-terminal and the downstream/carboxyl-terminal coding regions of *cyaD1* first were amplified using cyaD1Lb-chase2upRb and chase2downLb-cyaD1R as primers (Table S3) and then were digested with BamHI-NotI and NotI, respectively, and were ligated together. The resulting CHASE2-lacking DNA fragment was introduced between blunt-ended HindIII and BamHI sites of pDK5, generating the pDK5::*cyaD1ΔCHASE2* intermediate construct. The 1,130-bp KpnI-EcoRI fragment from pDK5::*cyaD1ΔCHASE2* was cloned into digested KpnI- and EcoRI-digested pBBR1MCS5, which replicates in both *E. coli* and *S. meliloti*, to yield pGIMI50127.

Similarly, the *clr*-expressing construct pGIMI50128 was obtained after PCR amplification of the *clr* gene-coding region using *S. meliloti 1021* genomic DNA as template and REco2175 and LBamH2175 as primers. The PCR fragment was digested with BamHI and EcoRI, ligated into a BamHI-EcoRI–digested pFAJ1708 plasmid, and introduced into *E. coli* DH5α by transformation. The verified plasmid was digested by XbaI and SstI and cloned into the XbaI-SacI–digested pBBRMcs5 plasmid to yield pGIMI50128.

To construct pGD2178, a 436-bp PCR fragment encompassing the *smc02178* promoter region was amplified using 2178B and 2178H primers, digested with BamH1 and HindIII, and cloned in the in-frame orientation at the same sites of the *lacZ* translational fusion plasmid pGD926.

All constructs were verified by PCR and Sanger sequencing in *E. coli* and by PCR in *S. meliloti*. Plasmids were transferred from *E. coli* to *S. meliloti* by triparental mating using pRK600 as the helper plasmid.

Plant Assays and Plant Extracts and Preparations. Seeds of *M. sativa* cv. Europe were surface sterilized, germinated, and allowed to grow in 12-cm² plates containing slanting nitrogen-free Fahraeus agar medium for 3 d at 22 °C with day/night cycles of 16/8 h. The plants then were inoculated with 2×10^3 bacteria per plant. *M. sativa* cv Gemini Nar variants were grown under aeroponic sterile conditions as described previously (31). Acetylene-reduction assays were performed as previously described 42 d after rhizobial inoculation (32).

For plant extract preparation, *M. sativa* seedlings growing on Fahraeus medium in squared plates were inoculated with either *S. meliloti 1021* or *exoY* mutant or were not inoculated. At 14 dpi, nodules, shoots, and non-nodulated portions of the roots of inoculated plants as well as roots and shoots of noninoculated plants were collected and frozen immediately in liquid nitrogen. Frozen nodules, roots, and shoots were crushed with a pestle in Eppendorf tubes, and the resulting material was resuspended in distilled water and centrifuged at $3,000 \times g$ for 8 min. The cleared supernatant was filtered through a 0.22-µm filter (Millipore) and stored at −80 °C, if needed, before assay. Nodule and/or shoot extracts of pea (*Pisum sativum* Cameor), lotus (*Lotus japonicus* GIFU), and rice (*Oryza sativa* Nippon Bare) were prepared similarly. *M. sativa* root exudates were prepared as previously described (33).

β-Galactosidase Assays. *S. meliloti* strains carrying the pGD2178 plasmid were grown at 28 °C in VGM. Overnight cultures were diluted to an OD$_{600}$ of 0.1 in VGM and grown for an additional 2 h. Cultures (10 mL) then were incubated in microoxic conditions as described (32) or were supplemented with 0.5 mL plant extracts, 1 mL of a 100-fold dilution of *Medicago* root exudates, 10 mM (final concentrations) of cAMP (A6885; Sigma), 10 µM luteolin (L9283; Sigma), 0.2% proline, 0.15 M sucrose, and 0.3 M NaCl and were grown for an additional 3 h or 24 h. β-Galactosidase activities were measured (in Miller units) using 1 mL of culture, as previously described (34). When plant tissue extracts were used as inducers, the measured activity was corrected for the background activity (i.e., activity of the fusion in absence of plant extract) and divided by the fresh weight of plant material used for the extract.

Cytological Techniques. Plants were inoculated with *S. meliloti* strains (wild-type and mutants) carrying the pXLGD4 replicative plasmid (Table S2) that expresses the *hemA-lacZ* reporter gene fusion constitutively. Entire roots were collected 7 dpi or 14 dpi, fixed with 2% (vol/vol) glutaraldehyde solution for 1.5 h under vacuum, rinsed three times in Z′ buffer [0.1 M potassium phosphate buffer (pH 7.4), 1 mM MgSO$_4$, and 10 mM KCl], and stained overnight at 28 °C under vacuum in Z′ buffer containing 0.08% 5-bromo-4-chloro-3-indolyl-β-D-galactoside (X-gal), 5 mM K$_3$Fe(CN)$_6$, and 5 mM K$_4$Fe(CN)$_6$. Nodules were harvested at 14 dpi, fixed with 2% (vol/vol) glutaraldehyde in Z′ buffer, and then sliced into 80-µm-thick longitudinal sections using a vibrating-blade microtome (VT1000S; Leica) before staining without vacuum overnight at 28 °C. Entire roots or nodule sections were observed under a light microscope.

cAMP and cGMP Measurements. The bacterial pellet obtained after centrifugation of a 20-mL early exponential phase culture of *S. meliloti* in M9 medium was washed with 0.9% NaCl and resuspended in 2 mL distilled water. Then 1 mL was used for protein quantification using the Bradford method (Bio-Rad), and 1 mL, supplemented with EDTA (4 mM final concentration), was boiled for 10 min and centrifuged. The resulting supernatant was lyophilized and stored at −20 °C until the test. The lyophilized samples were used to determine intracellular cAMP and cGMP levels with the enzyme immunoassay method according to the protocol given in Amersham kits RPN2251 for cAMP and RPN226 for cGMP.

Statistical Analysis. Data are presented as means ± SEM unless otherwise indicated. An unpaired, two-sided Student's *t* test was used when indicated.

1. Masson-Boivin C, Giraud E, Perret X, Batut J (2009) Establishing nitrogen-fixing symbiosis with legumes: How many rhizobium recipes? *Trends Microbiol* 17:458–466.
2. Madsen LH, et al. (2010) The molecular network governing nodule organogenesis and infection in the model legume Lotus japonicus. *Nature Communications* 1:10.1038/ncomms1009.
3. Oldroyd GED, Murray JD, Poole PS, Downie JA (2011) The rules of engagement in the legume-rhizobial symbiosis. *Annu Rev Genet* 45:119–144.
4. Long SR (2001) Genes and signals in the Rhizobium-legume symbiosis. *Plant Physiol* 125:69–72.
5. Gibson KE, Kobayashi H, Walker GC (2008) Molecular determinants of a symbiotic chronic infection. *Annu Rev Genet* 42:413–441.
6. Li DX, Kinkema M, Gresshoff PM (2009) Autoregulation of nodulation (AON) in *Pisum sativum* (pea) involves signalling events associated with both nodule primordia development and nitrogen fixation. *J Plant Physiol* 166:955–967.
7. Magori S, Kawaguchi M (2009) Long-distance control of nodulation: Molecules and models. *Mol Cell* 27:129–134.
8. Okamoto S, et al. (2009) Nod factor/nitrate-induced CLE genes that drive HAR1-mediated systemic regulation of nodulation. *Plant Cell Physiol* 50:67–77.
9. Murray JD, et al. (2007) A cytokinin perception mutant colonized by Rhizobium in the absence of nodule organogenesis. *Science* 315:101–104.
10. Penmetsa RV, Cook DR (1997) A legume ethylene-insensitive mutant hyperinfected by its rhizobial symbiont. *Science* 275:527–530.
11. Vernie T, et al. (2008) EFD Is an erf transcription factor involved in the control of nodule number and differentiation in *Medicago truncatula*. *The Plant Cell* 20:2696–2713.
12. Van de Velde W, et al. (2010) Plant peptides govern terminal differentiation of bacteria in symbiosis. *Science* 327:1122–1126.
13. Galibert F, et al. (2001) The composite genome of the legume symbiont Sinorhizobium meliloti. *Science* 293:668–672.
14. Zhulin IB, Nikolskaya AN, Galperin MY (2003) Common extracellular sensory domains in transmembrane receptors for diverse signal transduction pathways in Bacteria and Archaea. *J Bacteriol* 185:285–294.
15. Linder JU (2006) Class III adenylyl cyclases: Molecular mechanisms of catalysis and regulation. *Cell Mol Life Sci* 63:1736–1751.
16. Marden JN, Dong QA, Roychowdhury S, Berleman JE, Bauer CE (2011) Cyclic GMP controls *Rhodospirillum centenum* cyst development. *Mol Microbiol* 79:600–615.
17. Batut J, Daveran-Mingot ML, Jacobs MDJ, Garnerone AM, Kahn D (1989) FixK, a gene homologous with FNR and CRP from *Escherichia coli*, regulates nitrogen-fixation genes both positively and negatively in *Rhizobium meliloti*. *EMBO J* 8:1279–1286.
18. Terakado J, Fujihara S, Yoneyama T (2003) Changes in cyclic nucleotides during nodule formation. *Soil Sci Plant Nutr* 49:459–462.
19. Soupene E, Foussard M, Boistard P, Truchet G, Batut J (1995) Oxygen as a key developmental regulator of *Rhizobium meliloti* N2-fixation gene expression within the alfalfa root nodule. *Proc Natl Acad Sci USA* 92:3759–3763.
20. Truchet G, et al. (1989) Alfalfa nodulation in the absence of Rhizobium. *Mol Gen Genet* 219:65–68.
21. Cheng HP, Walker GC (1998) Succinoglycan is required for initiation and elongation of infection threads during nodulation of alfalfa by *Rhizobium meliloti*. *J Bacteriol* 180:5183–5191.
22. Capela D, Filipe C, Bobilk C, Batut J, Bruand C (2006) *Sinorhizobium meliloti* differentiation during symbiosis with alfalfa: A transcriptomic dissection. *Mol Plant Microbe Interact* 19:363–372.
23. Gage DJ (2004) Infection and invasion of roots by symbiotic, nitrogen-fixing rhizobia during nodulation of temperate legumes. *Microbiol Mol Biol Rev* 68:280–300.
24. Batut J, Mergaert P, Masson-Boivin C (2011) Peptide signalling in the rhizobium-legume symbiosis. *Curr Opin Microbiol* 14:181–187.
25. Jarnaess E, Tasken K (2007) Spatiotemporal control of cAMP signalling processes by anchored signalling complexes. *Biochem Soc Trans* 35:931–937.
26. McDonough KA, Rodriguez A (2011) The myriad roles of cyclic AMP in microbial pathogens: From signal to sword. *Nat Rev Microbiol* 10:27–38.
27. Becker A, et al. (2004) Global changes in gene expression in *Sinorhizobium meliloti* 1021 under microoxic and symbiotic conditions. *Mol Plant Microbe Interact* 17:292–303.
28. Dephilip P, Batut J, Boistard P (1990) *Rhizobium meliloti* FixL is an oxygen sensor and regulates *Rhizobium meliloti* nifA and fixK genes differently in *Escherichia coli*. *J Bacteriol* 172:4255–4262.
29. Oke V, Long SR (1999) Bacteroid formation in the Rhizobium-legume symbiosis. *Curr Opin Microbiol* 2:641–646.
30. Marx CJ, Lidstrom ME (2002) Broad-host-range cre-lox system for antibiotic marker recycling in Gram-negative bacteria. *Biotechniques* 33:1062–1067.
31. Ampe F, Kiss E, Sabourdy F, Batut J (2003) Transcriptome analysis of *Sinorhizobium meliloti* during symbiosis. *Genome Biol* 4:R15.
32. Bobik C, Meilhoc E, Batut J (2006) FixJ: A major regulator of the oxygen limitation response and late symbiotic functions of *Sinorhizobium meliloti*. *J Bacteriol* 188:4890–4902.
33. Mulligan JT, Long SR (1985) Induction of *Rhizobium meliloti* nodC expression by plant exudate requires NodD. *Proc Natl Acad Sci USA* 82:6609–6613.
34. Miller G (1972) *Experiments in Molecular Genetics* (Cold Spring Harbor Laboratory, Cold Spring Harbor, NY).